

Search for H I emission from superdisk candidates associated with radio galaxies

Abhijeet Anand¹, Nirupam Roy² and Gopal-Krishna^{3,4,*}

¹ Max-Planck-Institut für Astrophysik, Karl-Schwarzschild-Str. 1, D-85741 Garching, Germany;
abhijeet@mpa-garching.mpg.de

² Department of Physics, Indian Institute of Science, Bangalore - 560012, India

³ Aryabhata Research Institute of Observational Sciences (ARIES), Manora Peak, Nainital - 263129, India

⁴ Max-Planck-Institut für Radioastronomie, Auf dem Hügel 69, 53121 Bonn, Germany

Received 2018 October 29; accepted 2018 December 11

Abstract Giant gaseous layers (termed “superdisks”) have been hypothesized in the past to account for the strip-like radio emission gap (or straight-edged central brightness depression) observed between twin radio lobes, in over a dozen relatively nearby powerful Fanaroff-Riley Class II radio galaxies. They could also provide a plausible alternative explanation for a range of observations. Although a number of explanations have been proposed for the origin of the superdisks, little is known about their material content. Some X-ray observations of superdisk candidates indicate the presence of hot gas, but a cool dusty medium also seems to be common. If they are entirely or partly composed of neutral gas, then it may be directly detectable and we report here a first attempt to detect/image any neutral hydrogen gas present in the superdisks that are inferred to be present in four nearby radio galaxies. We have not found a positive H I signal in any of the four sources, resulting in tight upper limits on the H I number density in the postulated superdisks, estimated directly from the central rms noise values of the final radio continuum subtracted image. The estimated ranges of the upper limit on neutral hydrogen *number density* and *column density* are $10^{-4} - 10^{-3}$ atoms per cm^3 and $10^{19} - 10^{20}$ atoms per cm^2 , respectively. No positive H I signal is detected even after combining all the four available H I images (with inverse variance weighting). This clearly rules out an H I dominated superdisk as a viable model to explain these structures, however, the possibility of a superdisk being composed of warm/hot gas still remains open.

Key words: galaxies: active — galaxies: general — galaxies: structure — radio lines: galaxies

1 INTRODUCTION

Conspicuous radio emission gaps with sharp, quasi-linear edges have been noticed in the middle of the twin radio lobes of nearly 20 powerful double radio sources. These strip-like emission gaps (or sharp-edged brightness depressions), oriented roughly orthogonally to the axis defined by the radio lobe pair, have a typical width of about 30 kpc and length of at least 50–100 kpc, and are suspected to be caused due to a giant layer of thermal gas enveloping the massive elliptical galaxy hosting the double radio source (Gopal-Krishna & Wiita 1996, 2000; Gopal-Krishna et al. 2007; Gopal-Krishna & Wiita 2009). As argued in these papers, such postulated *superdisks* can provide viable alternative explanations to a range of well known phenom-

ena associated with radio galaxies and quasars, namely (i) the radio lobe depolarization asymmetry, popularly known as the Laing-Garrington effect (Laing 1988; Garrington et al. 1988); (ii) correlated radio-optical asymmetry of double radio sources (McCarthy et al. 1991); (iii) the occurrence of absorption dips in the Lyman- α (Ly- α) emission profiles of high- z radio galaxies with a total radio extent of up to ~ 50 kpc (van Ojik et al. 1997; Binette et al. 2006); and (iv) the apparent asymmetry of the extended Ly- α emission found associated with the lobes of high- z radio galaxies (Gopal-Krishna & Wiita 2000, hereafter GKW2000). Since the sharp edges of the radio brightness gaps/depressions would only be conspicuous when the axis of the double radio source is oriented near the plane of the sky and hence the twin radio lobes do not appear par-

* Visiting Professor, ARIES

tially overlapping, the (inferred) superdisks probably exist in many more radio galaxies than are actually observed.

Although the postulated superdisks (or ‘fat-pancakes’) might play a significant role in causing several well-known correlations exhibited by radio galaxies, as mentioned above, progress in understanding their nature is severely hampered due to the lack of information about their content. Early hints for the presence of dusty material in the superdisks emerged from the observed asymmetry of the extended Ly- α emission in high- z radio galaxies and from the above cited correlated radio-optical asymmetry (GKW2000 and references therein). Such a cool component (with dusty clumps) would also be consistent with the curious result (van Ojik et al. 1997; Binette et al. 2006) that absorption dips in the Ly- α emission profiles of radio galaxies are mostly seen when the overall radio extent of the lobes is under ~ 50 kpc, i.e., comparable to the typical width of the putative superdisks (Gopal-Krishna & Wiita 1996, 2000, 2009). An observation particularly relevant to the superdisk hypothesis is the detection of an enormous H I ring (with diameter ~ 200 kpc) surrounding an early-type galaxy NGC 612 hosting a double radio source (Emonts et al. 2008, and references therein). Although a superdisk signature is not evident in the radio images of this particular radio galaxy, this could be understood if the aforementioned requirement of the radio axis lying close to the sky plane remains unsatisfied in this case.

Motivated by the aforementioned findings and correlations, a number of physical scenarios have been proposed wherein the superdisks are envisioned to be: (a) a layer of dusty neutral and/or ionized gas blocking (at least partially) the backflow of synchrotron plasma from the radio lobes, which is the tidally stretched remnant of a disk galaxy captured by the elliptical galaxy that hosts the double radio source (Gopal-Krishna & Nath 1997, see also, Black et al. 1992); (b) a thermal wind bubble blown by the accretion disk of the active galactic nucleus (AGN), which is sandwiched and compressed by the backflowing synchrotron plasma from the twin radio lobes (Gopal-Krishna et al. 2007); (c) a segment of the gaseous filaments from the cosmic web in which the galaxy hosting the radio source happens to reside (Gopal-Krishna & Wiita 2000, 2009). In this scheme, the putative superdisks must have already existed prior to the birth of the double radio source (see also, Hardcastle et al. 2007); (d) in a radically different scenario, superdisks are carved out as two galaxy cores, each containing a supermassive black hole (SMBH), merge and the associated pair of relativistic plasma jets undergoes a rapid precession during the later stage of the merger (Gergely & Biermann 2009). Some additional mechanisms proposed for the origin of superdisks are mentioned in Section 4.

While the different proposed scenarios seem plausible, the choice of leading contender(s) is contingent upon a direct detection of the putative superdisks, possibly in emission. With the aim to address this critical information deficit, we have performed a sensitive search for H I emission from four nearby Fanaroff-Riley Class II (FR-II; Fanaroff & Riley 1974) radio galaxies whose high-resolution maps show that the twin radio lobes have a nearly straight edge on the side facing the host galaxy, thus marking a strip-like radio emission gap between the lobe pair (Table 1). It is worth pointing out that although the existence of a ‘superdisk’ is not established through direct observations, we are not aware of any satisfactory alternative explanation for the observational results/correlations mentioned in Section 1. These four radio galaxies were selected from the first sample of ten superdisk candidates (GKW2000), which was assembled through a visual inspection of the then available radio galaxy images. The selected four galaxies are among the nearest ones in the sample.

As an example, in Figure 1 we display one of them (3C 227). The grey scale image and radio brightness profile are taken along the major radio axis. The sharply bounded central brightness depression marks the location of the superdisk inferred to be associated with this source (see also Baum et al. 1988, Black et al. 1992 and ‘An Atlas of DRAGNs’¹ edited by J. P. Leahy, A. H. Bridle & R. G. Strom, for high resolution radio continuum images of these sources). To the best of our knowledge, no targeted H I observations of superdisk candidate radio galaxies had been carried out prior to the ones reported here.

It may be noted that out of the 10 radio galaxies listed in GKW2000 that are deemed to possess superdisks, five lie at $z < 0.1$. Here we report on the H I search for four of these five radio galaxies. The fifth source (3C 33) could not be observed due to scheduling considerations. The observational details of this project are provided in Section 2. In Section 3, we present the results. After a brief discussion, our main conclusions are summarized in Section 4.

2 OBSERVATIONS AND DATA ANALYSIS

The four superdisk candidates in radio galaxies ($0.03 < z < 0.09$) were observed during January to March, 2013, with the NSF’s Karl G. Jansky Very Large Array (VLA) in its D-configuration, yielding a baseline coverage from 0.035 to 1.03 km (VLA Project code 13A-194). The total observation time was 11 hours including the calibration and other overheads (total 5 h including 4 h on-source for 3C 227, and a total of 2 h including 1.5 h on-source for each of the remaining three sources).

¹ <http://www.jb.man.ac.uk/atlas/>

Table 1 Basic Parameters of the Target Radio Galaxies (GKW2000)

Source	Coordinates		Redshift (z)	D_A (Mpc)	D_L (Mpc)	Superdisk size ^g		FWHM of the synthesized beam
	R.A. (J2000)	Dec. (J2000)				d (kpc)	w (kpc)	
3C 98	03 ^h 58 ^m 54.0 ^s	10°26′03″	0.0304 ^a	126.5 ^d	134.3 ^d	30	15	56.3″ × 46.7″
3C 192	08 ^h 05 ^m 34.9 ^s	24°09′50″	0.0597 ^b	239.5 ^d	269.0 ^d	80	25	76.6″ × 46.5″
4C+32.25	08 ^h 31 ^m 27.5 ^s	32°19′26″	0.0512 ^a	207.5 ^f	229.3 ^f	150	52	55.2″ × 41.5″
3C 227	09 ^h 47 ^m 45.0 ^s	07°25′20″	0.0858 ^{c,e}	334.0 ^f	393.8 ^f	85	33	59.5″ × 50.7″

(i) Name, (ii) Coordinates, (iii) Redshift, (iv) Distance (angular dia. distance D_A and luminosity distance D_L), (v) Inferred superdisk size (minimum dia. d and width w), and (vi) Full width at half maximum (FWHM) of the synthesized beam (see Fig. 3).

Refs: [a] Massaro et al. (2015); [b] Argudo-Fernández et al. (2015); [c] Oh et al. (2015); [d] Leahy et al. (1997); [e] Black et al. (1992); [f] Wright (2006); [g] GKW2000.

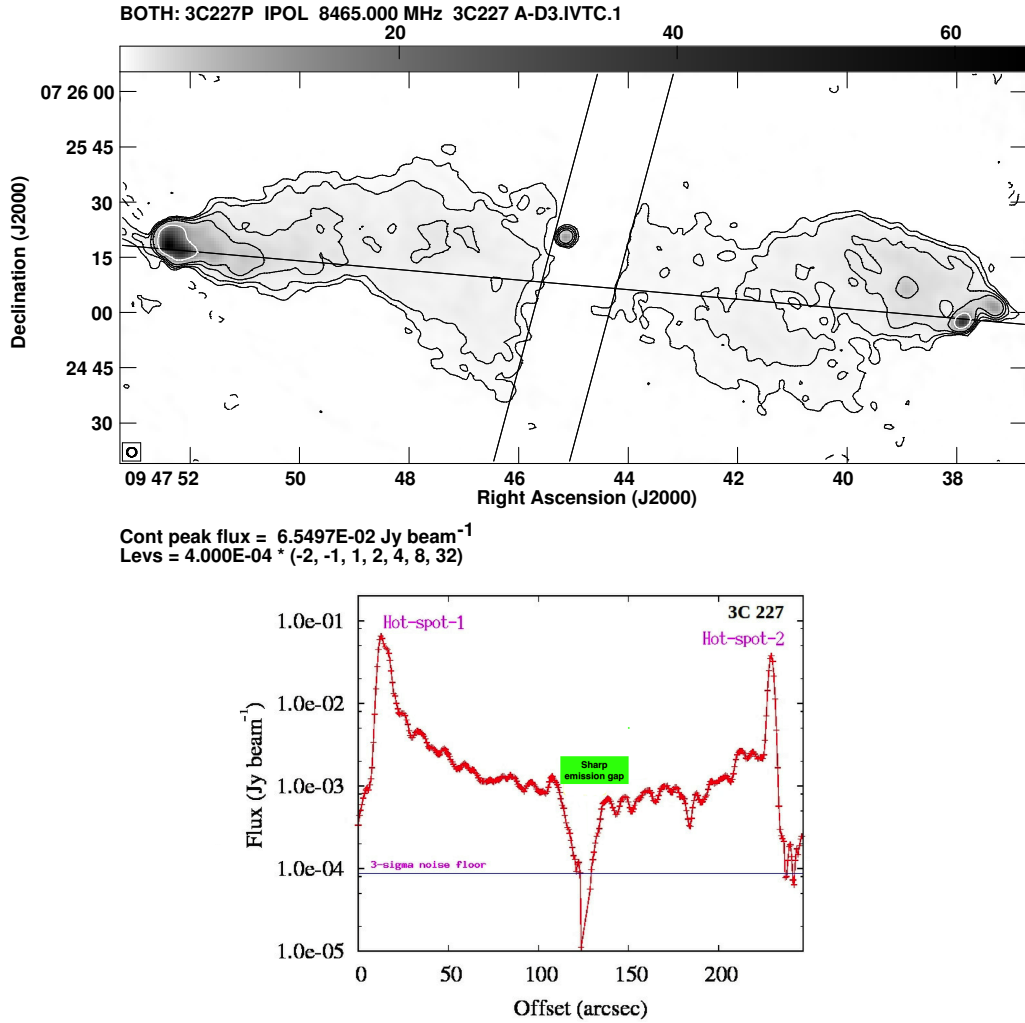


Fig. 1 *Top*: VLA X-band (8.4 GHz) grey scale image with $(-2, -1, 1, 2, 4, 8, 32) \times 3\sigma$ contours of superdisk candidate 3C 227 (with available data from Black et al. 1992). The two parallel lines overplotted delineate the region of radio emission gap. *Bottom*: 8.4 GHz radio emission profile of the same source along the axis joining the two hotspots, also overplotted on the top panel image, clearly displays the sharp emission gap.

To achieve a reasonable sensitivity and uv -coverage, the observations were carried out with a bandwidth of 16 MHz centered at the redshifted H I frequency and using 512 spectral channels. This yielded an overall veloc-

ity width of $\sim 3500 \text{ km s}^{-1}$ at a spectral resolution of $\sim 7 \text{ km s}^{-1}$. The relatively high spectral resolution enabled a more effective radio frequency interference (RFI) flagging. We opted for a large velocity coverage considering the to-

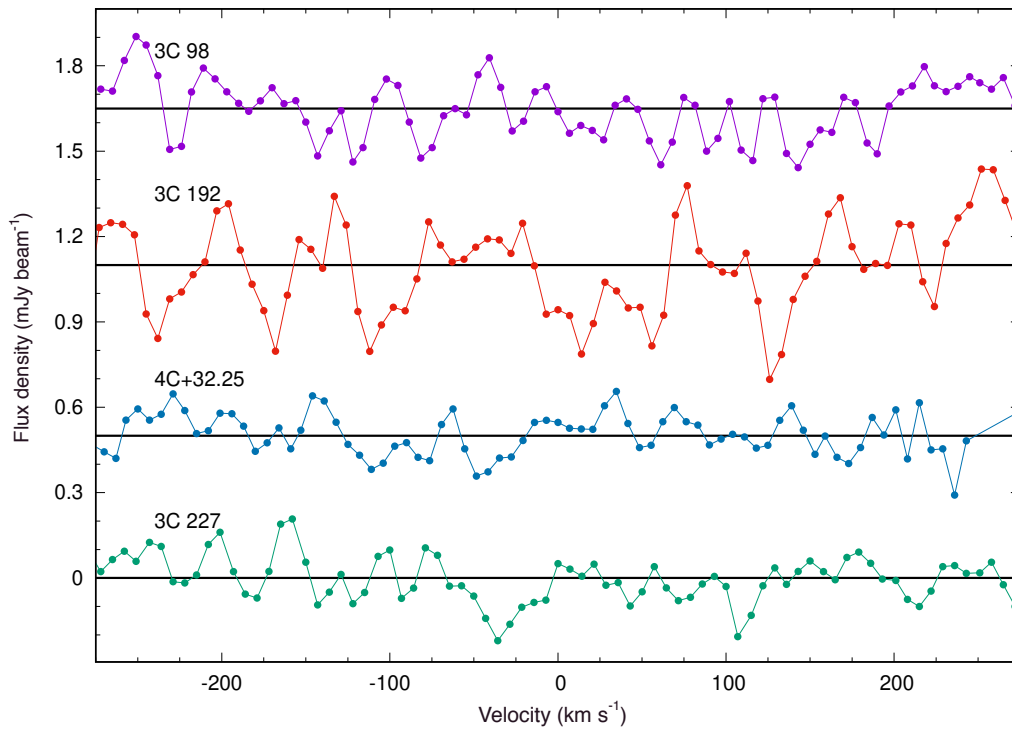


Fig. 2 The final continuum subtracted spectra for the four superdisk candidates, with a velocity resolution of $\sim 7 \text{ km s}^{-1}$. The spectrum for the 3C 227 superdisk is a combination of the spectra derived from its observations on the two days. Note that, for clarity, the spectra have been shifted vertically.

tal lack of *a priori* information about the width of the putative H I emission line. The 512 channels provided enough “line-free” (and RFI-free) channels to be able to properly subtract the continuum and thus establish a flat spectral baseline. The data reduction was done in the Common Astronomy Software Applications (CASA) package version 4.6.0 (McMullin et al. 2007) and the Astronomical Image Processing System (AIPS) version 31DEC17 (van Moorsel et al. 1996) following standard procedures. As a consistency check, the initial flagging and calibration for one of the targets (namely, 3C 98) were carried out both manually and using the VLA Scripted Calibration Pipeline version 1.3.8 (McMullin et al. 2007). Subsequently, for flagging and calibration of the rest of the data, we only used the pipeline. Additional data flagging, initial imaging and self-calibration of the continuum data, and the final continuum imaging were done using AIPS. The AIPS task UVSUB was then employed to subtract the continuum, CVEL to accurately convert the observed frequency to Heliocentric velocity, and thereafter, IMAGR was run on the residual data to generate image cubes at various spectral resolutions. Residual spectral baseline was removed by applying the task IMLIN on the spectral data cube. Finally, we visually inspected the cube for any emission signatures and to extract the spectrum of the central radio emission gap. For 3C 227, the data from the two observing sessions were analyzed separately and then combined with inverse

variance weighting at the final stage subsequent to the continuum subtraction.

3 RESULTS

Despite a fairly high sensitivity, the present VLA observations have not yielded a positive signal of H I 21 cm emission from any of the four superdisk candidates. Figure 2 displays the spectra extracted at their locations, for a $\pm 300 \text{ km s}^{-1}$ velocity range, at the original spectral resolution. Even when the spectral cubes were smoothed to a resolution of $\sim 100 \text{ km s}^{-1}$, no significant signal of H I emission was detected for any of the four targets (Fig. 3). The cross in each panel shows the central position of the emission gap at which the spectrum was extracted. We note that even after a careful flagging, calibration and imaging, there are some residual low-level artifacts, probably due to *uv*-coverage limitations or residual RFI in some of the images. However, they do not significantly affect the central region from where the spectra have been extracted. We set the 3σ noise as the upper limit to H I mass under the assumptions of optically thin line emission (Draine 2011) and a line width of 100 km s^{-1} . We then used the estimated size of the putative superdisk (Table 1) to compute the corresponding upper limit to H I number density and (averaged) H I column density (by a spatial averaging performed over the inferred superdisk region). These results

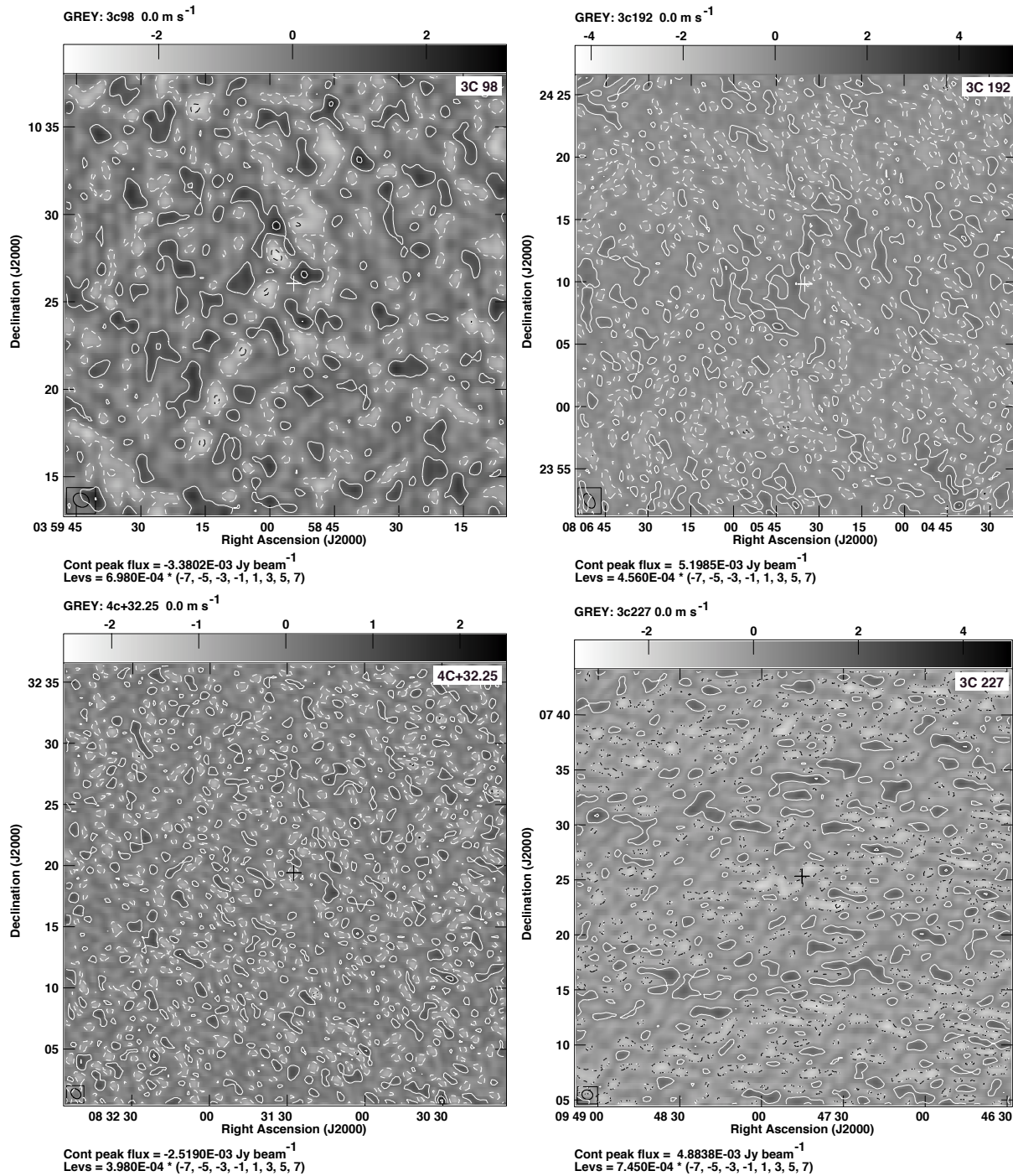


Fig. 3 The final continuum subtracted images with $\pm(1,3,5,7)\sigma$ contours overplotted, at the redshifted H I 21 cm frequency. The signal has been averaged over 100 km s^{-1} velocity bins. The brightness scale is indicated at the top of each plot. The central cross in each panel indicates the position of the nucleus of the radio source. Values for the FWHM of the synthesized beam, shown within the inset in each image, are $56.3'' \times 46.7''$ (3C 98), $76.6'' \times 46.5''$ (3C 192), $55.2'' \times 41.5''$ (4C+32.25) and $59.5'' \times 50.7''$ (3C 227).

are summarized in Table 2. It should be remembered that the size estimate for each superdisk is quite approximate, as the superdisk may extend even beyond the lateral extent of the radio emission gap. In each case, the spatial resolution of the present observations is such that the synthesized beam size is very similar to the size of the emission

gap and hence the beam should encompass much of the putative superdisk. Lastly, in a bid to further enhance the sensitivity, we have combined the final four H I images, all smoothed to a common resolution of $76.6'' \times 76.6''$ (the largest among the synthesized beams for the four sources), with inverse variance weighting. However, as seen from

Table 2 The 3σ upper limits to the H I number density, column density and mass of the putative superdisks in the four observed radio galaxies, assuming a velocity width of $\sim 100 \text{ km s}^{-1}$.

Source	rms noise ($\mu\text{Jy beam}^{-1}$)	$\langle n(\text{H I}) \rangle$ (cm^{-3})	$\langle N(\text{H I}) \rangle$ (cm^{-2})	$M(\text{H I})$ (M_{\odot})
3C 98	698	1.6×10^{-3}	1.5×10^{20}	4.2×10^8
3C 192	456	3.5×10^{-4}	8.7×10^{19}	1.1×10^9
4C+32.25	398	2.4×10^{-4}	1.1×10^{20}	5.4×10^9
3C 227	745	7.1×10^{-4}	1.9×10^{20}	3.3×10^9

Note that the listed rms noise values refer to the velocity width resulting from spectral smoothing over 15 channels, in order to obtain a velocity resolution of 100 km s^{-1} . These are $\sim 5 - 10$ times above the confusion level in the D configuration for VLA L-band observations ($74 \mu\text{Jy beam}^{-1}$).

Figure 4, even this stacking of the H I spectra for the four superdisk candidates has not yielded a significant H I signal.

4 SUMMARY AND DISCUSSION

The present VLA H I imaging observations have provided the first information on the H I content of the putative superdisks. For this, we have carried out H I imaging targeting a sample of four nearby radio galaxies in which a superdisk has been inferred on the basis of high-resolution radio continuum maps (Table 1; Section 1). Although the derived upper limits to H I mass ($10^8 - 10^9 M_{\odot}$) for these superdisks are similar to the H I content of the Milky Way, the corresponding average H I number densities have upper limits of only $10^{-4} - 10^{-3}$ atoms per cm^3 , thanks to the immense volumes of the inferred superdisks. We reiterate that the superdisk dimensions adopted here are approximate because they only refer to the region of the strip-like radio emission gap (or brightness depression) seen between the radio lobe pair; in reality the superdisk may extend well beyond the lobe width, resulting in even tighter upper limits on H I number densities. Considering this, upper limits on the average H I *column density* might be more meaningful (Table 2). Thus, while extension of H I searches to more superdisk candidates and to deeper levels would be very desirable, the present study does point to a scarcity of H I in superdisks, the highly suggestive evidence for dust in superdisks notwithstanding (Section 1). Here it may be mentioned that the presence of dust or dusty globules/filaments, per se, does not rule out a superdisk medium dominated by a warm/hot gas. For instance, dust emission has been convincingly detected in the central parts of the X-ray emitting clusters of galaxies (e.g., Yamada & Kitayama 2005; Montier & Giard 2005; Kitayama et al. 2009). It is also important to clarify that our observations do not exclude the existence of a small, kpc-scale H I disk in these galaxies. For comparison, the typical H I column density of such disks can be of the order of $0.6 - 3.1 \times 10^{19}$ atoms per

cm^2 (Serra et al. 2012), which would remain undetected with the surface-brightness sensitivity of the present wide-beam images targeting much larger H I structures (i.e., superdisks) that are postulated to explain the observed huge radio emission gaps. The present observations only imply that the volume density of H I in the putative superdisks must be at least an order of magnitude lower than that estimated for the kpc-scale H I disks seen in some early-type galaxies (e.g., Serra et al. 2012).

One class of gaseous structures that might have some bearing on the superdisk scenario is the so called ‘‘gas belts’’ (Mannering et al. 2013, and references therein). These X-ray detected structures have been identified in a few radio galaxies located in group/cluster-like environments, namely 3C 35 (Mannering et al. 2013), 3C 285 (Hardcastle et al. 2007), 3C 386 (Duffy et al. 2016) and 3C 442A (Hardcastle et al. 2007; Worrall et al. 2007). The belt-like structures of hot gas associated with these radio galaxies are seen to broadly overlap with the radio gap/depression between their twin radio lobes and are oriented roughly orthogonally to the axis defined by the radio lobe pair. No consensus has yet emerged about their formation mechanism. Hardcastle et al. (2007) argued that the central X-ray ridge, i.e., the gas belt, in 3C 285 is a ridge of thermal plasma that pre-existed the commencement of the radio activity, an inference which was also reached in Gopal-Krishna & Wiita (2009), from the observed greater lobe-length symmetry when measured relative to the mid-plane of the superdisk, rather than when referenced to the host galaxy. On the other hand, for the case of 3C 442A, Worrall et al. (2007) argued that the gas belt is the hot gas being stripped from the merging galaxies and is getting aligned into a belt shape as it pushes the twin radio lobes straddling it (see also, Gopal-Krishna et al. 2007, for a scenario involving a dynamical interaction of the hot thermal gaseous halo with the radio lobe pair). Yet another explanation, advanced by Mannering et al. (2013) for the case of 3C 35, posits that its gas belt has formed out of the gas belonging to the fossil galaxy group but driven outward due to the expansion of the twin radio lobes. More recently, a temperature gradient has been detected along the projected 53 kpc length of the gas belt observed in 3C 386, with a cooler gas core ($T \sim 0.73 \pm 0.09 \text{ keV}$) found closer to the host elliptical and hotter ($T \sim 1.72 \pm 0.46 \text{ keV}$) outer portion of the belt interpreted as the group’s atmosphere which is undergoing an inward flow triggered by the buoyant rise of the twin radio lobes through the circumgalactic medium (Duffy et al. 2016). While all these physical processes may be operating to varying degrees, the striking straightness of the lobes’ brightness contours marking the edges of the central radio emission gap/depression, which we identify as a superdisk, continues to pose a challenge

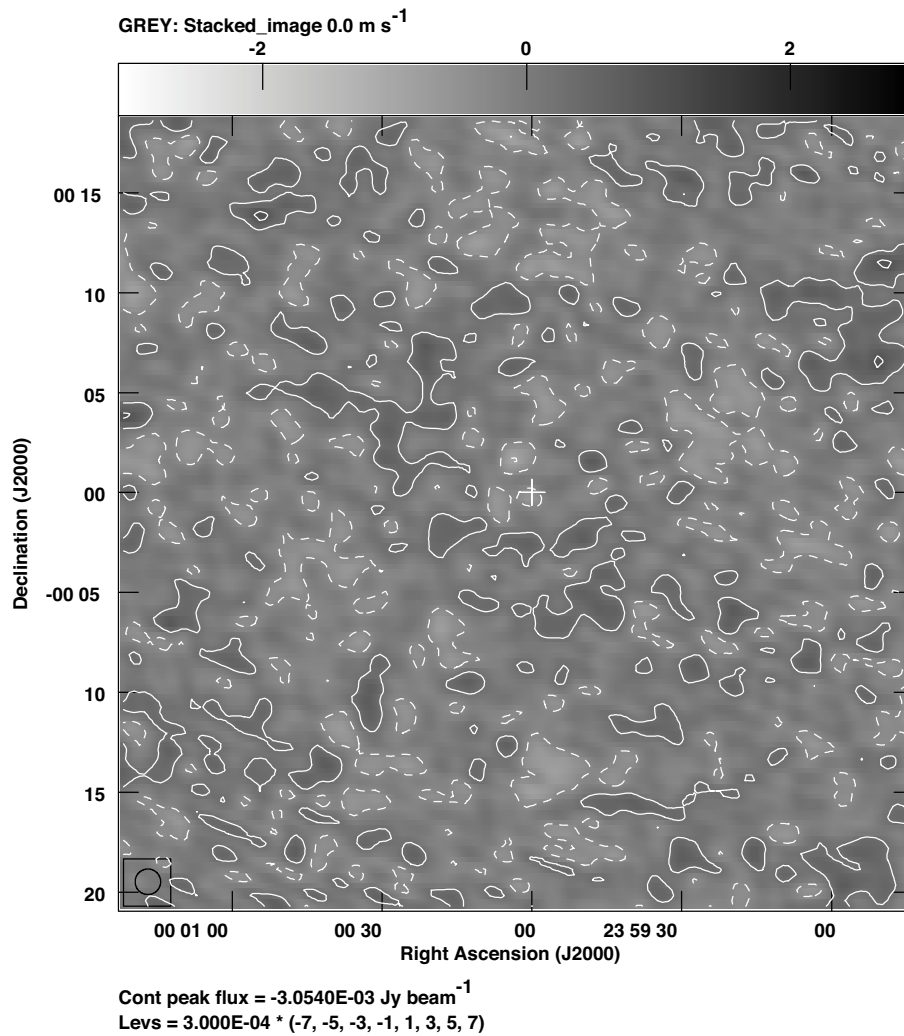


Fig. 4 Stacked H I image of the four superdisk candidates, each smoothed to a $76.6'' \times 76.6''$ beam and then combined with inverse variance weighting, after aligning at the redshifted H I 21 cm frequency and averaging over 100 km s^{-1} velocity bins. The grey scale image is overplotted with $\pm(1, 3, 5, 7)\sigma$ contours of the H I signal. The scale is indicated at the top. The root mean square (rms) noise in the combined map is $0.3 \text{ mJy beam}^{-1}$ and the inset shows the FWHM of the restored synthesized beam.

and its origin remains to be properly understood. Perhaps even more enigmatic are the several radio galaxies, highlighted in Gopal-Krishna & Wiita (2009), where the host elliptical galaxy is located nearly at one edge of the strip-like central radio depression (i.e., superdisk), or even *outside* it, i.e., within a radio lobe (this puzzling extreme situation is witnessed in the radio galaxy 3C 16, e.g., Harvanek & Hardcastle 1998). Since superdisks are likely to contain both ionized and dusty cool gas, a multi-pronged observational follow-up will be important, including the possibility of H I search through sensitive absorption measurements against any available background radio source.

Acknowledgements We are grateful to Eric Greisen, Sanjay Bhatnagar, Arnab Rai Choudhuri and Prateek Sharma for useful discussions. This research has made use of NASA’s Astrophysics Data System. The results reported

here are based on observations acquired with the Karl G. Jansky Very Large Array of the National Radio Astronomy Observatory. The National Radio Astronomy Observatory is a facility of the National Science Foundation operated under cooperative agreement by Associated Universities, Inc. Most of the work was done when AA was at the Indian Institute of Science as an undergraduate student. NR acknowledges support from the Infosys Foundation through the Young Investigator grant. G-K thanks the Alexander von-Humboldt Foundation for financial support and Prof. A. Zensus, Director of the Max-Planck-Institut für Radioastronomie, Bonn for the local hospitality.

References

Argudo-Fernández, M., Verley, S., Bergond, G., et al. 2015, *A&A*, 578, A110

- Baum, S. A., Heckman, T. M., Bridle, A., van Breugel, W. J. M., & Miley, G. K. 1988, *ApJS*, 68, 643
- Binette, L., Wilman, R. J., Villar-Martín, M., et al. 2006, *A&A*, 459, 31
- Black, A. R. S., Baum, S. A., Leahy, J. P., et al. 1992, *MNRAS*, 256, 186
- Draine, B. T. 2011, *Physics of the Interstellar and Intergalactic Medium* (Princeton Univ. Press)
- Duffy, R. T., Worrall, D. M., Birkinshaw, M., & Kraft, R. P. 2016, *MNRAS*, 459, 4508
- Emonts, B. H. C., Morganti, R., Oosterloo, T. A., et al. 2008, *MNRAS*, 387, 197
- Fanaroff, B. L., & Riley, J. M. 1974, *MNRAS*, 167, 31P
- Garrington, S. T., Leahy, J. P., Conway, R. G., & Laing, R. A. 1988, *Nature*, 331, 147
- Gergely, L. Á., & Biermann, P. L. 2009, *ApJ*, 697, 1621
- Gopal-Krishna, & Nath, B. B. 1997, *A&A*, 326, 45
- Gopal-Krishna, & Wiita, P. J. 1996, *ApJ*, 467, 191
- Gopal-Krishna, & Wiita, P. J. 2000, *ApJ*, 529, 189
- Gopal-Krishna, & Wiita, P. J. 2009, *New Astron.*, 14, 51
- Gopal-Krishna, Wiita, P. J., & Joshi, S. 2007, *MNRAS*, 380, 703
- Hardcastle, M. J., Kraft, R. P., Worrall, D. M., et al. 2007, *ApJ*, 662, 166
- Harvanek, M., & Hardcastle, M. J. 1998, *ApJS*, 119, 25
- Kitayama, T., Ito, Y., Okada, Y., et al. 2009, *ApJ*, 695, 1191
- Laing, R. A. 1988, *Nature*, 331, 149
- Leahy, J. P., Black, A. R. S., Dennett-Thorpe, J., et al. 1997, *MNRAS*, 291, 20
- Mannering, E., Worrall, D. M., & Birkinshaw, M. 2013, *MNRAS*, 431, 858
- Massaro, F., Harris, D. E., Liuzzo, E., et al. 2015, *ApJS*, 220, 5
- McCarthy, P. J., van Breugel, W., & Kapahi, V. K. 1991, *ApJ*, 371, 478
- McMullin, J. P., Waters, B., Schiebel, D., Young, W., & Golap, K. 2007, in *Astronomical Society of the Pacific Conference Series*, 376, *Astronomical Data Analysis Software and Systems XVI*, eds. R. A. Shaw, F. Hill, & D. J. Bell, 127
- Montier, L. A., & Giard, M. 2005, *A&A*, 439, 35
- Oh, K., Yi, S. K., Schawinski, K., et al. 2015, *ApJS*, 219, 1
- Serra, P., Oosterloo, T., Morganti, R., et al. 2012, *MNRAS*, 422, 1835
- van Moorsel, G., Kembell, A., & Greisen, E. 1996, in *Astronomical Society of the Pacific Conference Series*, 101, *Astronomical Data Analysis Software and Systems V*, eds. G. H. Jacoby, & J. Barnes, 37
- van Ojik, R., Roettgering, H. J. A., Miley, G. K., & Hunstead, R. W. 1997, *A&A*, 317, 358
- Worrall, D. M., Birkinshaw, M., Kraft, R. P., & Hardcastle, M. J. 2007, *ApJ*, 658, L79
- Wright, E. L. 2006, *PASP*, 118, 1711
- Yamada, K., & Kitayama, T. 2005, *PASJ*, 57, 611